Application of Quasi-static Method of Moments for the Design of Microwave Integrated Circuits and Antennas

Chun-Wen Paul Huang, Samir Hammadi, Jeannick Sercu*, Jian-Wen Bao, and Shihab Kuran

Anadigics, Inc., 35 Technology Drive, Warren, New Jersey, 07059, USA
*Agilent Technologies, EEsof EDA, Lammerstraat 20, 9000 Ghent, Belgium

I. INTRODUCTION

With the recent advancements in computer-aided design (CAD) technology, circuit simulators are being capable of simulating complex designs in a reasonably short time. To reduce the design cycle and development costs, design simulation is becoming a necessity for today's microwave and millimeter wave (mmW) integrated circuit (IC) designs. Besides operating at microwave and mmW frequencies, those designs are fairly complex. Accurate prediction of circuit performance before fabrication becomes a must for shortening design cycles and for lowering engineering cost. High-speed digital fiber optic integrated circuits, such as OC-192 (10 Gbit/s) and OC-768 (40 Gbit/s) are broadband circuits. They operate at frequencies ranging from the kHz range to a minimum of 10 GHz and from the kHz range to a minimum of 40 GHz, respectively. Such bandwidths are required to maintain low signal distortion levels. Therefore, accurate design simulations not only rely on the accuracy and robustness of transistor models, but also the passive layout models. These required models are due to the parasitic inductance, transmission line effects of the interconnections, and resonance of capacitors and inductors above microwave frequencies. Recently, several papers described the application of electromagnetic (EM) analysis tools for the design of the layouts in millimeter wave integrated circuits [1], [2]. However, these applications are limited to circuits of low complexity or periodic structures. For complicated circuits, the parasitic extraction method is widely applied to model the layouts of complicated IC's [3], that provides fast results and reasonable accuracy. However, it is difficult for parasitic extraction tools to model the resonance of capacitors and inductors at microwave frequencies, transmission line effects, and the air-bridge crossover capacitance [4]. Incomplete consideration of layout effects may result in peaking and sagging in the bandwidth of wideband circuits. A global circuit/layout modeling technique, based on the 2.5-D planar quasi-static Method of Moments (MoM) [5], [6], was presented and validated experimentally for its effectiveness for mmW IC applications in [7]. In this paper, the theory of quasi-static MoM is reviewed and presented for completeness. Comparative analyses of quasi-static MoM and conventional MoM approaches including convergence speed enhancements and computational requirements are also presented. The global layout analysis method in conjunction with vertical bipolar inter-company (VBIC) transistor models is applied to a complicated 10-Gbit/s broadband amplifier (see Fig. 1). Excellent agreements between simulated and measured results are observed in both frequency and time domains. Applications of quasi-Static MoM for microwave antenna designs are also presented. This method provides the first-order solutions of antenna resonance in a short computational time. Based on the fast quasi-static solutions, refined simulations with full-wave simulations for accurate bandwidths and radiation pattern analysis at specific frequencies can be made, which greatly shortens design cycle.

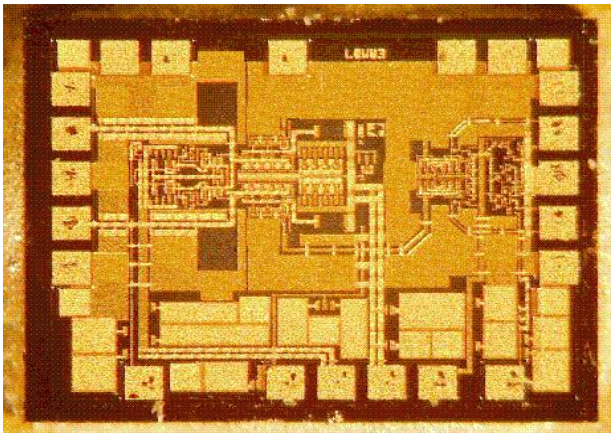

Fig. 1. OC-192 (10 Gbit/s) GaAs Amplifier.

II. FORMULATION OF QUASI-STATIC METHOD OF MOMENTS

The quasi-static Method of Moment technique was partially presented in [5], [6], and later the methodology was adopted in Agilent's EEsof Momentum RF [8]. In

this section, the theory of quasi-static MoM for free space problems is presented for completeness. This review is an expansion from the work presented in [5], [6]. This method is based on Mixed Potential Integral Equations. The relationship between the Mixed Potential Moment Matrix ([Z(ω)]) and the unknown currents |I(ω)> can be expressed as

$$[\mathrm{Z}(\omega)]\left|\mathrm{I}(\omega)\right\rangle = \left|\mathrm{V}(\omega)\right\rangle \tag{1}$$

where |V (ω)> is the voltage impressed by the sources or subject to the boundary conditions. The Moment Matrix can be re-expressed as,

$$[\mathrm{Z}(\omega)] = [\mathrm{R}(\omega)] + \mathrm{j}\omega[\mathrm{L}(\omega)] + 1/\mathrm{j}\omega\,[\mathrm{C}(\omega)]^{-1} \tag{2}$$

where [R (ω)], [L (ω)], and [C (ω)] represent the frequency dependent resistance, inductance, and capacitance matrices, respectively. A full-wave MoM can be developed based on equations (1) and (2). The explicit forms of the elements in [R (ω)], L [(ω)], and [C (ω)] matrices can be expressed in equations (3) to (5) as shown,

$$\begin{aligned} Z_{ij}^{R} &= R_{ij}(\omega) \\ &= Z_s(\omega)\iint_{S_i} ds \iint_{S_j} ds'\ \delta(\mathbf{r}-\mathbf{r}')\ \mathbf{B}_i(\mathbf{r})\cdot\mathbf{B}_j(\mathbf{r}') \end{aligned} \tag{3}$$

$$\begin{aligned} Z_{ij}^{L} &= j\omega L_{ij}(\omega) \\ &= \iint_{S_i} ds \iint_{S_j} ds'\ \mathrm{G_m}(\omega,\mathbf{r}-\mathbf{r}')\ \mathbf{B}_i(\mathbf{r})\cdot\mathbf{B}_j(\mathbf{r}'), \end{aligned} \tag{4}$$

$$\begin{aligned} Z_{ij}^{C} &= 1/\,j\omega C_{ij}(\omega) \\ &= \iint_{S_i} ds \iint_{S_j} ds'\,\mathrm{G_e}(\omega,\mathbf{r}-\mathbf{r}')\ \nabla\cdot\mathbf{B}_i(\mathbf{r})\ \nabla\cdot\mathbf{B}_j(\mathbf{r}'), \end{aligned} \tag{5}$$

where G (ω, **r-r'**) and **B(r)** are the Green's and the basis functions, respectively. The Green's function can be expressed in a Taylor series as,

$$G(\omega,\mathrm{r},\mathrm{r}') = e^{-jkR}/R = \tfrac{1}{R}\left(1 - jkR - (kR)^2/2! \cdots\right) \tag{6}$$

where k is the free-space wave number and R = |r-r'|. At low frequencies or when the structures are electrically small, the higher order terms in (6), that govern radiation, can be ingored. The quasi-static Green's functions can be expressed as,

$$G(\mathrm{r},\mathrm{r}') \approx \frac{1}{R}. \tag{7}$$

Based on equation (7), equations (4) and (5) can be simplified to obtain frequency scalable expressions. Therefore, the Moment matrix equation (2) can be simplified as

$$[\mathrm{Z}(\omega)] = [\mathrm{R}(\omega)] + \mathrm{j}\omega[\mathrm{L}] + 1/\mathrm{j}\omega\,[\mathrm{C}]^{-1}. \tag{8}$$

Instead of re-computing the entire Moment Matrix at each frequency, equation (8) provides a scalable Moment matrix, which greatly reduces the computational time. The maximum usable frequency is computed based on the requirement that the diagonal (D) of the structure is less than half of the free-space wavelength of the maximum frequency. The expression for the maximum frequency is

$$f_{\max} < \frac{150}{D(mm)}. \tag{9}$$

From equation (8), at low frequency the impedance matrix will tend to break down due to a zero of the inductive impedance matrix and an infinite capacitive impedance matrix. Therefore, instead of using traditional rooftop basis functions, the loop and star basis functions are adopted to ensure low frequency stability and enable mesh reduction [5], [6]. These features ensure shorter computational time and less memory requirements for complicated structures, in comparison with traditional 2.5-D full-wave MoM.

III. GLOBAL CIRCUIT/LAYOUT MODELING TECHNIQUES

The quasi-static MoM provides faster results and requires less memory, which enables EM modeling of complex IC layouts. The layout simulation is done using Agilent's Momentum RF and the circuit simulation is done by Agilent's Advanced Design System (ADS). Custom programs were built to integrate the layout tool, circuit simulator, and EM simulator for the global circuit/layout modeling. The technique is explained in this section. By setting up the layer mapping protocols, the circuit layouts can be correctly transferred between the layout tool and the EM simulator via Graphic Data System II (GDSII) or other standard layout data files. When modeling a layout, all transistors and resistors are removed in the layout tool by the custom programs. Transistors and resistors will be modeled in the circuit simulator with VBIC and transmission line models, respectively. Because the required computational time is a function of number of the unknowns square, the custom programs also enable the layout tool to generate layout partitions of a complicated layout to reduce the computational time. Partitioned layouts are exported to the EM simulator for layout modeling. After partitioned layouts are modeled, the EM simulator exports multi-port S-parameter layout models with look-alike symbols into the circuit simulator for circuit/layout co-simulations. When modeling a complicated layout, the layout models should be partitioned based on the coupling effects between the circuit stages and

elements. It is inadequate just to partition the layout based on the boundaries of circuit functional stages. One has to look at the coupling effects between various stages due to layout proximity. For this, the current visualization is an excellent vehicle for tracing the lines of minimum coupling. This coupling analysis is done using a global current visualization of a layout section using a low meshing density (shown in Fig. 2). Multiple ports were used in the layout simulation to emulate the current distribution around the transistor cells. The brighter color traces indicate higher EM coupling density, and the darker region indicates the low coupling between traces. This provides fast, first order results for the coupling effects. The partitioned layout models are simulated with fine meshing resolution. For modeling IC passive circuitry and interconnections, the meshing frequency and density need to be higher than those for the RF board and antenna applications to generate adequate current samples for small IC traces.

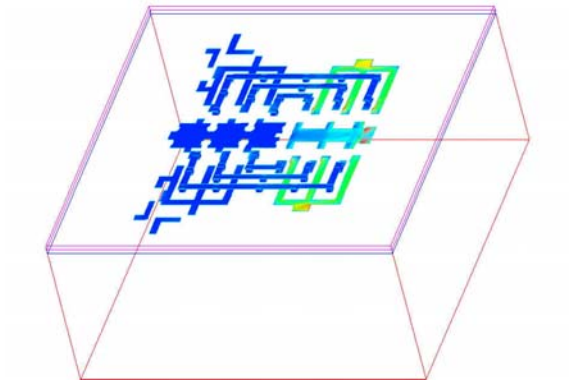

Fig. 2. Global visualization of induced currents between interconnections for the localization of layout modeling.

IV. VALIDATION FOR MICROWAVE CIRCUITS AND ANTENNA APPLICATIONS

Most quasi-static methods are used for modeling low frequency or electrically short structures. In this section, the quasi-static MoM is validated for modeling millimeter wave IC passive circuitry, a complex microwave IC, and electrically long structures. Its extended applications for the predictions the resonances of microwave antennas of arbitrary shapes are also presented. Analyses of the computational time and memory versus traditional MoM are also provided.

A. OC-768 Millimeter Wave IC Applications

For the OC-768 application, integrated circuits are required to operate at 40 Gbit/s. Therefore, the IC passive circuitry is also an important part of IC designs. Two examples are presented and verified with measurements. Modeling skills using quasi-static MoM at mmW IC passive are also presented.

Two 1.9-mm coplanar waveguides are printed side by side with a 50 μm separation on an Indium Phosphide (InP) wafer, shown in Fig. 3(a). The electrical lengths of waveguides are similar to those of typical traveling wave amplifiers (TWA) for OC-768 applications. The waveguide is filled with Benzocyclobutene (BCB) low dielectric material, which has a dielectric constant of 2.7 and loss tangent of 0.008. To accurately model a CPW with mmW with 2.5-D EM simulator, the thick metal strip model, composed of top and bottom strips and a via, are used to emulate the side-wall effects of finite-thickness metal strips (see Fig. 3 (b))[9]. Dielectric 2 is the substrate InP and the dielectric 1 is the over-mold material, which is BCB in this example. The extracted Z_o of infinitely thin strip model is 82.7 Ω, which is overestimated compared with 69 Ω from the thick metal model. The effectiveness of the quasi-static MoM for millimeter Wave applications is observed in Fig. 4. The spikes in S-parameter magnitude measurements and simulations, found at 24 GHz, are caused by higher order modes, which are confirmed by inspecting the magnitudes and phases of the measured S-parameters of both waveguides. However, the resonances in the measurements are weaker than those in simulations. Hence, the effectiveness of the quasi-static MoM is validated.

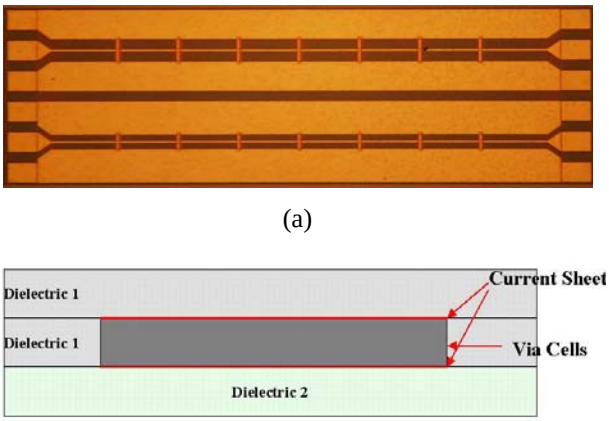

(a)

(b)

Fig. 3. (a) InP coplanar waveguides for OC-768 (40 Gbit/s) applications; (b) Thick metal model for a 2.5-D MoM simulator.

Table I shows the convergence of Z_o and R_{dc} for this example as a function of meshing density using Quasi-static MoM. Table II shows the required computational resources of the quasi-static MoM. Fast convergence and minimum computational requirements are observed compared with full-wave MoM. Both full-wave and quasi-static demonstrated the similar accuracy

compared with measurement shown in Table I. The quasi-static MoM requires 40 % to 90 % of the memory needed by the conventional 2.5 D MoM and simulates the circuit in 1/8 to 1/6 of the time. The relation between the computational time and memory requirements versus the unknown number (N) for quasi-static MoM can be expressed as follows

$$CPU \quad Time \quad = 5x10^{-6} N^{2.2}, \tag{10}$$

$$Memory \quad = 1.8x10^{-3} N^{1.47}. \tag{11}$$

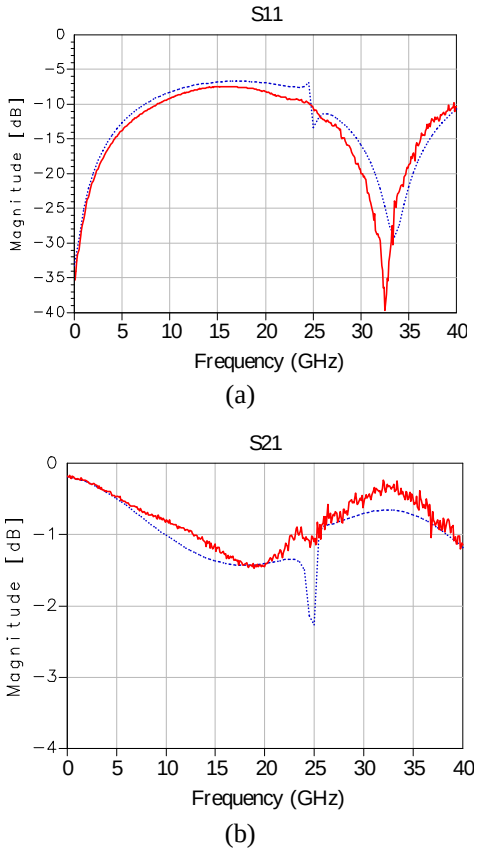

Fig. 4. Measurements (solid line) versus quasi-static MoM simulations (dotted line) (a) Return Loss (dB); (b) Insertion Loss (dB).

The relation between the computational time and memory requirements versus the unknown number (N) for a full-wave 2.5-D MoM can be expressed as follows

$$CPU \quad Time \quad = 1x10^{-6} N^{2..5}, \tag{12}$$

$$Memory \quad = 110e^{0.0002N}. \tag{13}$$

From Tables I and II, and equations (10) to (13), the computational speed improvement of quasi-static MoM is a result of both the reduction of the number of unknowns and the frequency scalable Moment matrix.

Another OC-768 application of a capacitive loaded electrode design of Electro-Optical Modulator [10] is also presented. As shown in Fig. 5 (a), the electrodes of the modulator are composed of a CPW with T-rail capacitors and two optical waveguides underneath the center conductor of the CPW. The Modulator is fabricated on a GaAs wafer with 1cm electrodes. To accurately characterize the electrically long and periodic electrodes, the electrodes were modeled in a 2 mm cell with extended feeds for S-parameter extraction. The GDSII file of the layout is imported into the EM simulator. The modeling method is similar to the previous example, and the thick metal strip model in the previous example was used to ensure the accuracy. The extended feeds are used to minimize the abrupt transitions at the excitation planes of the unit cell and provide more accurate S-parameter extractions. The 2 mm cell is about one wavelength at 40GHz, and the extended feeds are de-embedded from the simulated S-parameters. Comparisons of the simulated and measured phase velocity (V_{ph}), characteristic impedance (Z_o), and attenuation are shown in Fig. 5 (b). Excellent agreements between simulation and measurements are observed.

For electrically long transmission structures, the division of layout models should be made based on the localized coupling effects and appropriate electrical length. EM models of both examples have electrical lengths more than a half wavelength. The characteristics of both structures are determined by transmission

Table I. Convergence Test of Quasi-static MoM.

Mesh Density (cell/λ @ 40 GHz)	5	15	25	50
Zo @ 40 GHz (Measured Zo = 70.6 Ω)	72	69.7	69.2	69.1
R @ DC (Measure R = 2.02 Ω)	2.3	2.29	2.20	2.12

Table II. Quasi-Static MoM (RF) versus Full-wave MoM (MW) in Required Computational Resources on a 450 MHz Workstation.

Mesh Density (cell/λ @ 40 GHz)	5		15		25		50	
Type of MoM	RF	MW	RF	MW	RF	MW	RF	MW
Unknowns	1516	3054	1898	3515	2570	4332	4771	6988
Memory (MB)	90.37	216.65	119.98	218.60	195.69	269.75	416.91	488.64
CPU Time (min)	61.25	550.03	95.05	761.32	197.97	1300.53	785.74	4304.8

characteristics and localized couplings instead of far-end couplings. Therefore, quasi-static models for transmission structures can be used beyond the limit specified in equation (9). To re-confirm this statement, a 1.5 inch coupler is simulated and measured (see Fig. 6).

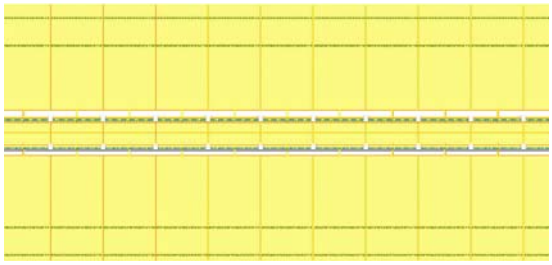

(a)

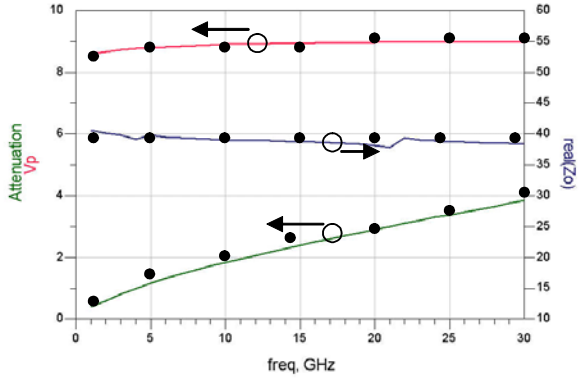

(b)

Fig. 5. (a) The top view of a 40 Gbit/s Electro-Optical Modulator; (b) Measurements (symbol) versus quasi-static MoM simulations (solid line) of electrode phase velocity (cm/ns), attenuation (dB/cm), and characteristic impedance (Ω).

The coupler is only terminated at the two diagonal ports, which results in the strongest coupling effects. Equation (9) indicates the maximum usable frequency of 3.71 GHz, but good agreement between measurement and simulation was observed up to 9 GHz (1.5 wavelength). This experiment shows that weak-radiating structures can be accurately characterized by quasi-static MoM model beyond the half-wave length limit in equation (9). Therefore, the effectiveness and efficiency of quasi-static MoM for millimeter wave IC applications are proven.

B. Complex Microwave IC Layout Modeling

The global layout analysis in conjunction with VBIC transistor models and transmission line resistor models is applied to a 10 Gbit/s fiber optic amplifier (Fig. 1). The layout model partitioning analysis is applied to the circuit layout. Cross-talk analysis of a gain-stage layout is shown in Fig. 2. The color densities at different regions show the intensities of electromagnetic field couplings. Fig. 2 indicates low cross-talk between the

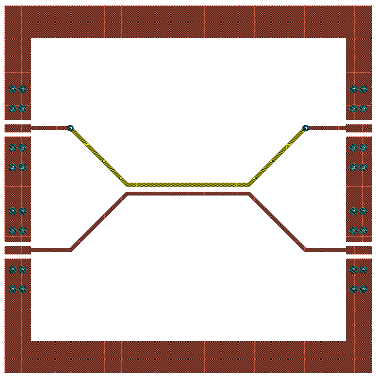

(a)

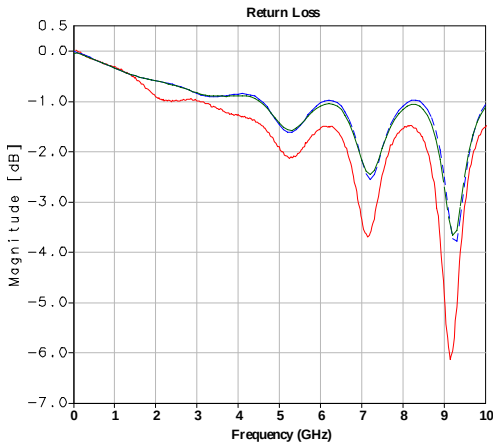

(b)

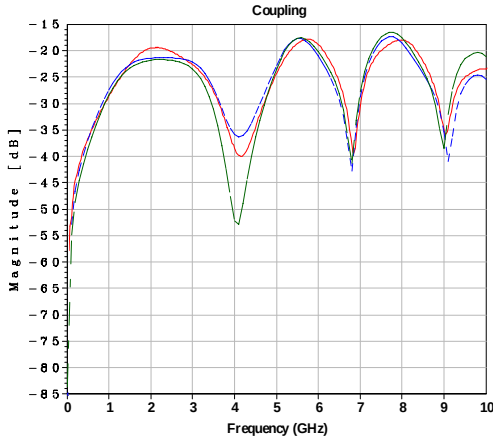

(c)

Fig. 6. Comparison of measured (solid line), full-wave 2.5-D MoM simulation (dash dot line), and quasi-static MoM simulation (dash line) of a 1.5-inch multilayer oupler. (a) Test structure; (b) Simulated and measured return loss; (c) Simulated and measured coupling.

two transistor arrays and hence the possibility of dividing this layout into two localized models. The transmitted and coupled current distributions were indicated by the color density of the visualization. The dark regions indicate low current distribution regions, and the brighter regions are indication the strong current crowdedness.

To support the circuit/EM co-simulation in fiber optic simulations, layout models are required for the low frequency stability, and the related elements can be biased with DC sources. Indeed, most EM simulators are incapable for accurate low frequency simulations. As previously indicated, the quasi-static MoM adopts the loop and star basis function instead of traditional rooftop basis function to ensure low frequency stability. In Fig. 7, a commonly used through-via multilayer interconnect is simulated with quasi-static and traditional full-wave MoM. The quasi-static MoM shows strong low frequency stability compared with full-wave MoM with rooftop basis functions. This feature provides the feasibility of bias through EM layout models and low frequency accuracy. Small signal validation is verified by comparing the magnitudes of the measured and simulated S-parameter results of the entire circuit, which is shown in Fig. 8.

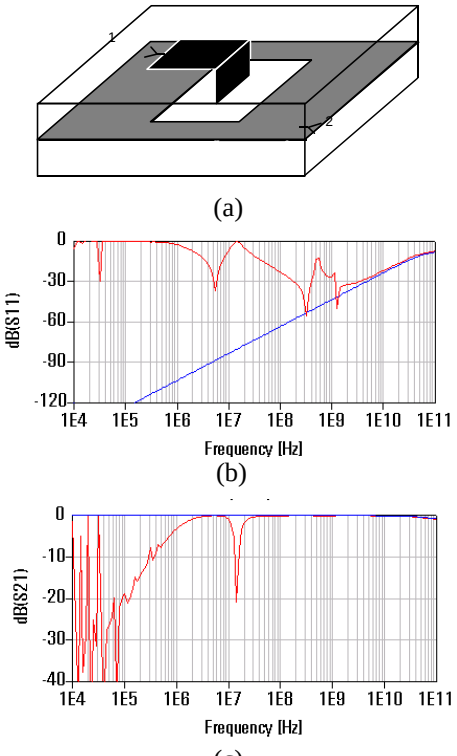

Fig. 7. Low frequency breakdown analysis of the rooftop basis function (solid line) and loop and star basis function (dotted line). (a) The test structure; (b) Simulated return Loss (dB); (c) Simulated insertion Loss (dB).

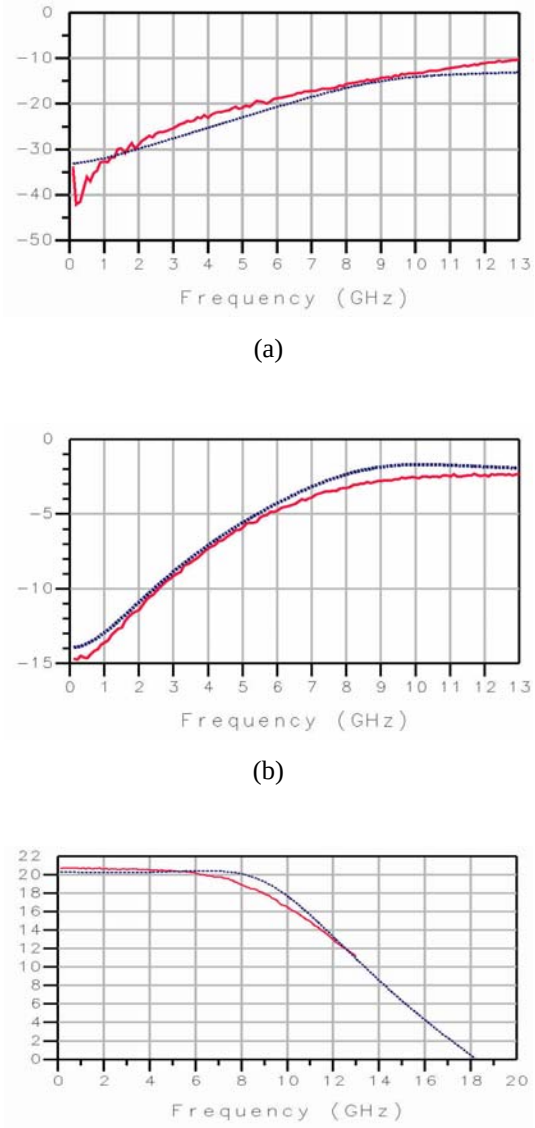

Fig. 8. Measured (solid line) versus simulated (dotted line) magnitudes of S-parameters for the OC-192 amplifier in Figure 3. (a) S11 (dB); (b) S22 (dB), and (c) S21 (dB).

To support time domain simulations of fiber optics circuits, sufficient frequency resolutions and maximum frequency are required based on the rise and fall time of the input pulse. For the 10 Gbit/s circuit simulations, a frequency resolution of 100 MHz and a maximum frequency of 20 GHz are used. Excellent agreement is observed. Large signal validation is verified by comparing transient simulation and measurement using eye diagrams, which is shown in Fig. 9. Good agreement in rise time, fall time and transient waveform is observed.

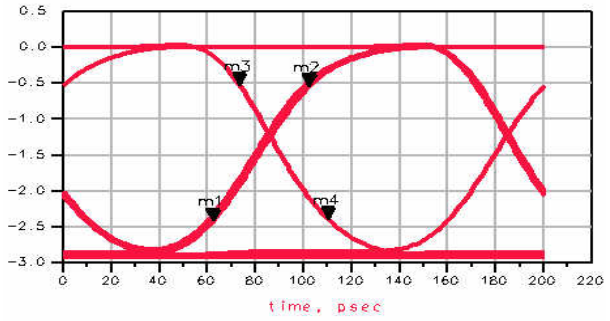

(a)

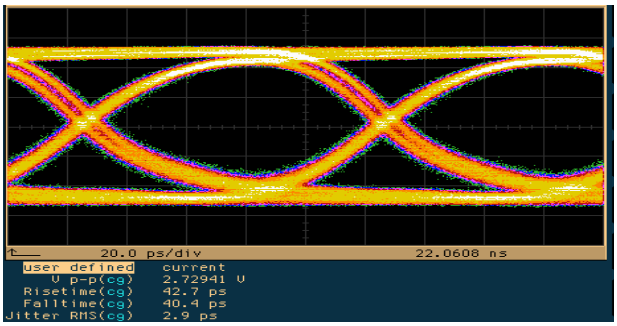

(b)

Fig. 9. Eye diagram of the 10Gbit/s GaAs amplifier. (a) Simulated eye diagram; (b) Measured eye diagram.

C. Predictions of Microwave Antenna Resonances

Equation (7) manifests the quasi-static assumption of neglecting the higher order terms in Greens' function, which enables the frequency scalable Moment matrix. However, the antenna impedance is mainly determined by the near fields instead of the far fields. Therefore, the quasi-static assumptions should is able to provide the first order solution of antenna resonances. Resonance frequencies, impedance bandwidths, and radiation pattern syntheses are the major antenna design parameters. For simple antenna structures, analytical solutions or simple numerical programs are often available. However, for designing antennas of arbitrary geometries, a more sophisticate numerical code is required to provide accurate results. Instead of using a full-wave EM simulator searching antenna operating modes within a wide bandwidth, the quasi-static MoM can predict the vicinities of antenna resonances in a much shorter computation time. Based on the quasi-static solutions, refined full-wave simulations for the impedance bandwidth and radiation pattern analyses within desired frequency bandwidths can be made. In this section, a ground backed planar antenna and a linear wire antenna were simulated and measured.

The first example is a circular patch antenna with a diameter of 4.22 cm printed on a 1.5 mm thick dielectric substrate with the permittivity of 2.55 [11]. This structure is simulated with both 2.5-D full wave and quasi-static MoM simulators. In [11], this antenna was measured from 4.9 to 5.5 GHz, at the vicinity of 3rd series resonance, which resonates at 5.18 GHz with 170 MHz operation bandwidth and antenna gain of 4.2 dB. The full-wave simulation for the antenna impedance bandwidth (see Fig. 10 (a) and (b)) shows agreement with the measurement in [11] but with a higher simulated gain of 4.6 dB. From Fig. 10 (a) and (b), quasi-static solutions predict the vicinities of usable resonances. The simulated impedance bandwidths of quasi-static MoM in Fig. 10 (a) provide relative levels, but the absolute values of impedance deviate from the full-wave simulations. The computational time for full-wave MoM is 86 minutes for 1541 unknowns, and the computational time for quasi-static MoM is 11 minutes for 958 unknowns. It is practical to use quasi-static MoM to locate the vicinities of usable antenna resonances.

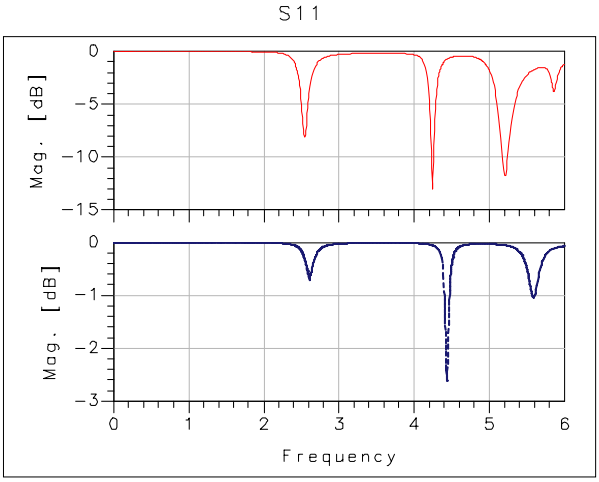

(a)

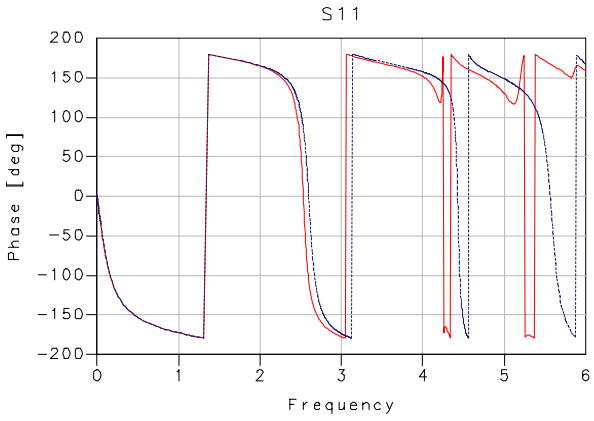

(b)

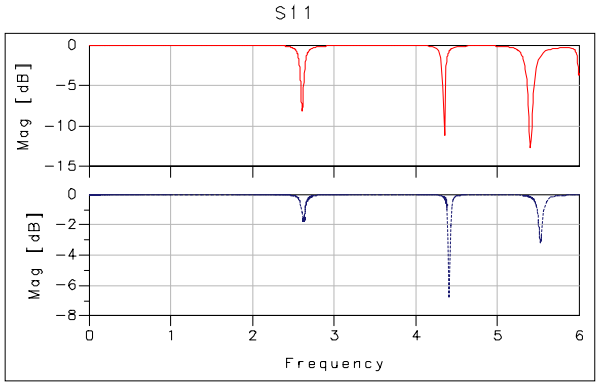

(c)

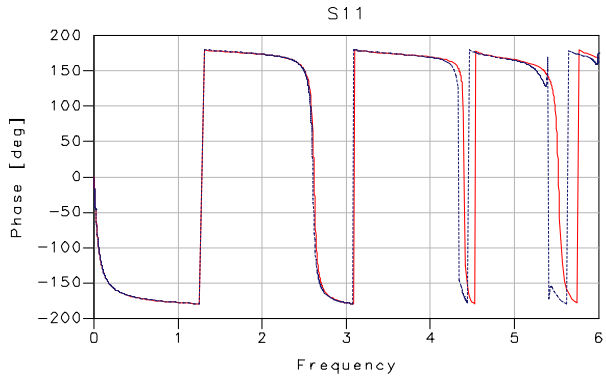

(d)

Fig. 10. Comparison of full-wave (solid line) and quasi-static (dash line) MoM simulations. Simulation of the circular patch antenna on a 1.5-mm thick substrate: (a) Magnitude of S11 and (b) Phase of S11. Comparison of full-wave (solid line) and quasi-static (dash line) MoM simulations. Simulation of the circular patch antenna on a 0.5-mm thick substrate: (c) Magnitude of S11 and (d) Phase of S11.

According to equation (9), the maximum frequency of quasi-static solution of this structure is 2.53 GHz, which also explains the deviation between full wave and quasi-static results increases after this frequency. When the substrate height is reduced from 1.5 mm to 0.5 mm, the agreement between full-wave and quasi-static simulations is improved shown in Fig. 10 (b). However, from full-wave simulations, the reduction of substrate thickness from 1.5 mm to 0.5 mm greatly decreases the radiation efficiency by 30 %.

The second example is a dual-sleeve meander line antenna (see Fig. 11 (a)), which is designed to operate at multiple operational modes [12]. The antenna is simulated and measured at an infinite ground plane. The quasi-static MoM captures the first 5 operational resonances. The impedance of this antenna is mainly determined by the mutual capacitance between segments, so the agreement is better than that of the ground-backed planar antennas. From Fig. 11, the full-wave solution shows better agreement with the measurement. However, the computational cost is much higher than quasi-static solutions. The required computational time of quasi-static MoM is 35 minutes for 978 unknowns, but the full-wave MoM requires 188 minutes for 1404 unknowns.

(a)

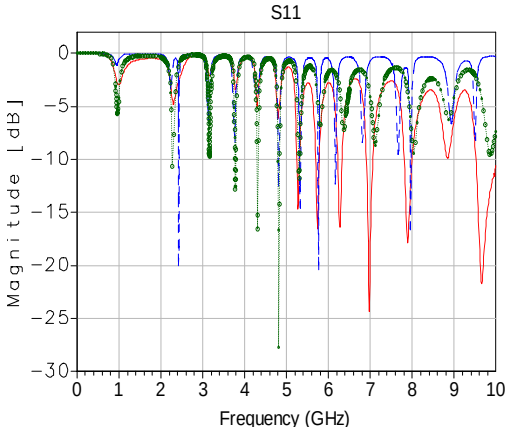

(b)

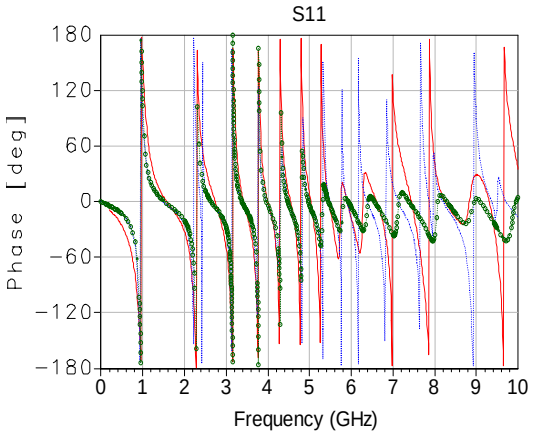

(c)

Fig. 11. Quasi-static (dash line) and full-wave (symbol) simulations versus measurement (solid line). (a) A dual-sleeve meander line antenna; (b) Magnitude of S11; (c) Phase of S11.

V. CONCLUSION

A novel global layout modeling technique based on a quasi-static MoM for complex IC designs is presented. The theory of quasi-static MoM is reviewed and its effectiveness and efficiency for microwave and millimeter wave IC applications is validated. This technique reduces the required memory size 10 to 60 % and decreases the simulation time by a factor of 6. Due to low radiation effects in MICROWAVE IC's, excellent agreement between simulated and measured results is observed. In addition, the low frequency stability of this method provides the accuracy of DC and wideband simulated results of EM/circuit model co-simulations, which is essential for complex microwave IC designs. Custom programs were generated to link layout CAD tool, the quasi-static MoM simulation engine, and a circuit simulator seamlessly, which greatly reduces design cycle. Effectiveness for modeling electrically long (>0.5 wavelength) structures is also proven. Its extended application for antenna resonance prediction is also presented, which provides the first order solutions for usable antenna resonances in a much shorter simulation time.

ACKNOWLEDGEMENT

The authors wish to express the appreciation to Dr. Charles E. Smith, the professor of the Electrical Engineering Department at The University of Mississippi, for his helpful technical discussions and Dr. Wei Zhong at Anadigics Inc. for providing the VBIC models.

REFERENCES

[1] J. W. Archer et al, "An InP MMIC amplifier for 180-205 GHz," *IEEE MICROWAVE and Wireless Comp. Letters*, vol. 11, no. 1, pp. 4-6, Jan. 2001.

[2] V. Radisic et al, "164-GHz MMIC HEMT Doubler," *IEEE MICROWAVE and Wireless Comp. Letters*, vol. 11, no. 6, pp. 241-243, Jun. 2001.

[3] W. H. Kao, C.-Y. Lo, M. Basel, R. Singh, "Parasitic extraction: current state of the art and future trends," *Proceedings of the IEEE*, vol. 89, no. 5, pp. 729-739, May 2001.

[4] T. M. Weller et al., "Three-Dimensional high-freuency distrubuted netowks, Part I: Optimiazation of CPW discontinuities," *IEEE Trans. Microwave Theory and Tech.*, vol. 48, no. 10, pp. 1635-1642, Oct. 2000.

[5] J. Sercu, "Inductance and capacitance modeling of RF board and high speed packaging interconnects based on planar EM simulation," *2nd MINT Millimeter-wave International Symposium*, Seoul, South Korea, Feb. 15-16, 2001.

[6] L. Knockaert, J. Sercu, and D. D. Zutter, "Generalized polygonal basis functions for the electromagnetics simulation of complex geometrical planar structures," *2001 IEEE International Microwave Symposium*, Phoenix, AZ, June 2001.

[7] C. P. Huang, J. Bao, N. Dwarakanath, and S. Al-Kuran, "Applications of quasi-static method of moments for the designs of OC-192 and OC-768 fiber optic integrated circuits," *IEEE 2002 RFIC Symposium*, pp. 97-100, June 2002.

[8] Agilent EEsof EDA, Advanced Design System 1.5 Momentum, Palo Alto, CA 94304, December 2000.

[9] C. P. Huang, S. Hammadi, J. Lott, and S. Al-Kuran, "Characterization of multiple-via interconnections for multilayer chip and module designs," *IEEE 2001 AP-S International Symposium*, July 2001.

[10] R. Spickermann, "High speed allium arsenide/aluminum gallium arsenide traveling wave electrop-optic modulators, *Ph.D. Dissertation, University of California at Santa Babara*, 1996.

[11] Y. J. Guo, A. Paez, R. A. Sadeghzadeh, and S. K. Barton, "A circular patch antenna for radio LAN's," *IEEE Trans. on Antennas and Propagation*, vol. 45, no. 1, pp. 177-178, Jan. 1997.

[12] C. P. Huang, A. Z. Elsherbeni and C. E. Smith, "Analysis and design of tapered meander line antennas for mobile communications," *Journal of Applied Computational Electromagnetics Society, Special Issue on Wireless Communications*, vol. 15, no. 3, pp. 159-166, 2000.